

Ion association in low-polarity solvents: comparisons between theory, simulation, and experiment

Chantal Valeriani,^{1,2} Philip J. Camp,^{3,*} Jos W. Zwanikken,^{4,5} René van Roij,⁴ and Marjolein Dijkstra²

¹*SUPA, School of Physics and Astronomy, The University of Edinburgh, Mayfield Road, Edinburgh EH9 3JZ, UK*

²*Soft Condensed Matter, Debye Institute for NanoMaterials Science, Utrecht University, Princetonplein 5, 3584 CC Utrecht, The Netherlands*

³*School of Chemistry, The University of Edinburgh, West Mains Road, Edinburgh EH9 3JJ, UK*

⁴*Institute for Theoretical Physics, Utrecht University, Leuvenlaan 4, 3584 CE Utrecht, The Netherlands*

⁵*Department of Material Science and Engineering, Northwestern University, 2220 Campus Drive, Evanston, Illinois 60208-3108, US*

(Dated: November 8, 2018)

The association of ions in electrolyte solutions at very low concentration and low temperature is studied using computer simulations and quasi-chemical ion-pairing theory. The specific case of the restricted primitive model (charged hard spheres) is considered. Specialised simulation techniques are employed that lead to efficient sampling of the arrangements and distributions of clusters and free ions, even at conditions corresponding to nanomolar solutions of simple salts in solvents with dielectric constants in the range 5-10, as used in recent experimental work on charged-colloid suspensions. A direct comparison is effected between theory and simulation using a variety of clustering criteria and theoretical approximations. It is shown that conventional distance-based cluster criteria can give erroneous results. A reliable set of theoretical and simulation estimators for the degree of association is proposed. The ion-pairing theory is then compared to experimental results for salt solutions in low-polarity solvents. The agreement is excellent, and on this basis some calculations are made for the screening lengths which will figure in the treatment of colloid-colloid interactions in such solutions. The accord with available experimental results is complete.

I. INTRODUCTION

The control of charged-colloid suspensions with added salt is a linchpin of soft condensed matter science. The physical principles that govern the net interactions between like-charged colloids in aqueous electrolyte solutions were laid down more than half a century ago.¹ Central to charge stabilization are the formation of the electrical double layer and the phenomenon of screening over distances comparable to the Debye length. The classic Derjaguin-Landau-Verwey-Overbeek and Debye-Hückel (DH) theories apply well to high-polarity solvents, such as water, where the electrostatic interactions between salt ions and counterions are strongly screened dielectrically. In particular, under normal conditions and with simple salts, cation-anion pairing is rather insignificant and complete ion dissociation can be assumed when describing the screening effect.

Charged colloidal suspensions in low dielectric constant solvents are now of experimental interest.²⁻¹¹ Such systems involve whole new regimes of low ion concentrations \sim nM, and strong electrostatic interactions between ions (added salt and counterions). The situation with regard to screening now changes because the reduction in dielectric screening compared to that in water can only enhance cation-anion association and promote the formation of a significant number of so-called Bjerrum pairs. This leads to a reduction in free ions and a concomitant increase in the screening length. The effects of ion pairing on the screening of colloidal interactions have been explored.¹²⁻¹⁴

Of course, ion pairing is not a new phenomenon, and its effects on the thermodynamics and dynamical properties can be highly pronounced.¹⁵ Already in 1926, Bjerrum described his eponymous pairs within a quasi-chemical ion-pairing equilibrium, and suggested removing them from the effective free-ion concentration when performing

DH-like calculations on electrolyte solutions.¹⁶ Bjerrum's theory has been thoroughly tested against experimental data for solutions with moderately low salt concentrations of $c_s \geq 10^{-5}$ M in solvents with dielectric constants in the range $2 \leq \epsilon \leq 80$.¹⁵ One of the most dramatic manifestations of ion pairing is in the phase separation of ionic fluids,^{17,18} where the low-concentration 'vapour' phase has such a high degree of ion association that the conventional DH theory has to be extended to include ion-dipole and dipole-dipole interactions in order to give a good account of accurate simulation data for the coexistence envelope.^{19,20}

From a computational perspective, the new experimental regimes of very low concentration and strong electrostatic interactions present some serious challenges. Molecular dynamics simulations of salts at nanomolar concentrations have already fallen foul of sampling problems.^{12,13} Recently, the current authors put forward a protocol for performing Monte Carlo (MC) simulations in the canonical ensemble, with novel particle moves that allow efficient equilibration at the extreme conditions referred to above.²¹ This opens up the opportunity to explore the true degree of association in very low concentration electrolyte solutions made up with low-polarity solvents. For the purposes of this exploratory study, attention is focused on the restricted primitive model (RPM) of ionic fluids. The RPM is an electroneutral mixture of $N/2$ positively and $N/2$ negatively charged hard spheres of equal diameter σ and charges $\pm q$ immersed in a dielectric continuum with dielectric constant ϵ and volume V at temperature T , with an overall ion concentration $\rho = N/V$. The interaction pair potential between ions i and j is

$$u(r_{ij}) = \begin{cases} \infty & r_{ij} < \sigma \\ \frac{q_i q_j}{D r_{ij}} & r_{ij} \geq \sigma \end{cases} \quad (1)$$

where r_{ij} is the pair separation, q_i is the charge on ion

i , and $D = 4\pi\epsilon_0\epsilon$ where ϵ_0 is the dielectric permittivity of vacuum. The overall ion concentration and temperature are given in reduced units by $\rho^* = \rho\sigma^3$ and $T^* = k_B T D \sigma / q^2$, respectively. The Bjerrum length is the distance at which the attractive cation-anion potential is equal to $-k_B T$, and is given by $\lambda_B = \sigma / T^*$. The phase behaviour of the RPM is now well known;^{22,23} the vapour-liquid critical parameters are $T_c^* \simeq 0.05$ and $\rho_c^* \simeq 0.08$.^{24,25} Simulations confirm that the degree of ion association in the vapour phase just below ρ_c^* and $T_c^* \simeq 0.05$ is significant.^{26–31} Indeed, the coexistence properties of fused cation-anion pairs (charged hard dumbbells) are almost identical to those of the RPM.^{32–34}

In this work, the degree of ion association in the RPM at very low concentrations and low (near-critical) temperatures is investigated. Calculations are performed down to a reduced ion concentration of $\rho^* = 10^{-10}$ and a reduced temperature of $T^* = 0.04$; for a monovalent salt with ionic diameter $\sigma = 4 \text{ \AA}$ at room temperature, these values correspond to a salt concentration $c_s \simeq 1 \text{ nM}$ and a solvent dielectric constant $\epsilon \simeq 5.6$. Using specialised MC simulations, results are obtained with which to test the quasi-chemical ion-pairing theory as proposed by Bjerrum. This involves using a novel simulation protocol recently proposed by us,²¹ and a variety of methods for determining the degree of association. The ion-pairing theory is then tested against experimental data for the degree of ion association; to this end, recent work by Lenissen and co-workers has yielded results for salts at concentrations of around 10^{-7} M in solvents with dielectric constants as low as about 5.^{10,35} To the best of our knowledge, this is the first time that a quantitative comparison has been made between theory, simulation, and experiment at such extreme conditions. On the basis of this comparison, the effects of ion association on the screening of charged-colloid interactions under such conditions can be evaluated with some confidence.

This article is arranged as follows. The ion-pairing theory is presented in Section II, and the simulation details are summarised in Section III. The RPM simulation results are given in Section IV A, and an analysis of experimental data is presented in Section IV B. Section V concludes the paper.

II. THEORY

To describe ion association, consider the quasi-chemical equilibrium



In terms of the degree of association α , the concentration of cation-anion pairs is $\rho_{\pm} = \alpha\rho/2$ and those of the cations and anions are $\rho_+ = \rho_- = (1 - \alpha)\rho/2$. Considering the mixture of cations, anions, and cation-anion pairs to be ideal, the chemical potentials are $\mu_{\pm} = k_B T \ln(\alpha\rho\Lambda_{\pm}^3\Lambda^3/2K)$, $\mu_+ = k_B T \ln[(1 - \alpha)\rho\Lambda_+^3/2]$, and $\mu_- = k_B T \ln[(1 - \alpha)\rho\Lambda_-^3/2]$, where Λ_+ and Λ_- are the de Broglie thermal wavelengths of the cations and anions, respectively. Here K is the configurational integral of a pair, which plays the role of an equilibrium constant:

$$K = 4\pi \int_{\sigma}^{r_c} r^2 \exp\left(\frac{\sigma}{rT^*}\right) dr. \quad (3)$$

The choice of the cutoff radius r_c is to be discussed below. At equilibrium $\mu_{\pm} = \mu_+ + \mu_-$, which leads to

$$\frac{\alpha}{(1 - \alpha)^2} = \frac{K\rho}{2}. \quad (4)$$

Solving for α yields

$$\alpha = 1 - \frac{1}{K\rho} \left(\sqrt{1 + 2K\rho} - 1 \right). \quad (5)$$

Considering the phase diagram of the RPM in the concentration-temperature plane, a sensible dividing line between ‘associated’ and ‘dissociated’ regimes is the locus of points defined by $\alpha = \frac{1}{2}$, or alternatively

$$K\rho = 4. \quad (6)$$

All that remains now is to determine the equilibrium constant K . The primary problem is that the integral in Eq. (3) does not converge for $r_c \rightarrow \infty$, and so in the conventional treatment, an appropriate finite upper limit for the integral needs to be identified. One choice for r_c is the Bjerrum length λ_B , on the basis that the separation between ions in a pair should be such that the interaction energy is greater in magnitude than $k_B T$. An alternative, and more conventional, choice is to set $r_c = \lambda_B/2$ corresponding to the minimum of the integrand $r^2 \exp(\lambda_B/r)$ in Eq. (3). It has long been recognised, however, that the precise choice of r_c is unimportant (see section 925 of Ref. 36), at least at low temperatures; this will be emphasised in the results of the current work. An approximate closed-form expression for K valid at low T^* can be obtained by noting that in a cation-anion pair, the separation r should not be much more than σ . Writing $r = \sigma + \delta r$ leads to the limiting behaviour $\sigma/r \approx 1 - \delta r/\sigma = 2 - r/\sigma$. Substituting this in to Eq. (3) and performing the integral with $r_c = \infty$ yields

$$K \approx 4\pi\sigma^3 e^{1/T^*} [T^* + 2(T^*)^2 + 2(T^*)^3]. \quad (7)$$

Equation (7) is possibly the most simple low-temperature result, and was inspired by a similar approximation for the two-particle partition function of dipolar hard spheres presented by Jordan;³⁷ the range of validity is limited by an unphysical minimum in K at $T^* \simeq 0.54$. Levin and Fisher have summarised several more accurate closed-form expressions.²⁰ Finally, it is acknowledged that Ebeling’s alternative expression for K ,³⁸ which reproduces the correct equation of state for the RPM up to terms of order $\rho^{5/2}$ and is therefore a more rigorous choice,²⁰ gives essentially identical results to the Bjerrum-length prescriptions employed here.

III. SIMULATION METHODS

Conventional MC simulations of associating fluids at very low concentrations can fail due to insufficient sampling of the most significant arrangements and spatial distributions of clusters.³⁹ On the one hand, during a typical length run using single-particle moves, isolated particles in very dilute systems may never come within sufficient proximity of other particles to associate. On the other hand, particles already within clusters may not be able

to detach due to it being a rare event. In an effort to eliminate these problems, the authors recently proposed an efficient MC protocol for simulating the RPM at very low concentrations and low temperatures where ion association is expected to be significant.²¹ The simulations are conducted within the canonical (NVT) ensemble using a cubic box of side $L = V^{1/3}$ with periodic boundary conditions. The long-range coulombic interactions are handled using the Ewald summation with conducting boundary conditions.⁴⁰ Various types of MC moves are attempted: normal single-particle moves with displacements chosen randomly from either a narrow interval (with a width adjusted to give an acceptance rate of 40%) or a broad interval (spanning the range $-L/2$ to $L/2$); cluster moves with displacements chosen randomly from narrow and broad intervals, as before; and ‘cluster formation/breakage’ (CFB) moves, each of which involves moving a second ion within a sphere of radius Δ centered on a randomly chosen first ion. This last move offers possibilities for bringing together two randomly selected isolated ions in to association, and for prising two clustered ions apart. Full details of the simulation protocol are reported in Ref. 21. The main control parameters are the radius Δ , and the various proportions of single-particle and cluster moves, small and large displacements, and CFB moves. On the basis of earlier work,²¹ the present simulations are performed with 70% small single-particle displacements, 10% large single-particle displacements, 5% small cluster displacements, 5% large cluster displacements, and 10% CFB moves. The CFB radius was set to $\Delta = L/4$ in all cases. These parameters were shown in Ref. 21 to give rapid convergence to the apparent equilibrium state. In all cases, the system is made up of $N = 256$ ions, and run lengths consist of 10^5 - 10^6 MC moves per ion, depending on density and temperature.

Conventionally, clusters in fluids are identified using some kind of pairwise distance²⁷ or energy-based criterion; the latter are useful for anisotropic potentials, where not only the distance but also the orientation have to be favorable for association to occur. In the present case, a distance-based criterion suffices; two particles are considered associated if their separation is less than some cutoff distance r_c . In their comprehensive study of ion association in the vapour phase of the RPM near coexistence, Caillol and Weis showed that the cluster distribution is basically independent of criteria in the range $1.8\sigma \leq r_c \leq 2.2\sigma$.⁴¹ Allahyarov *et al.* use $r_c = \lambda_B$ in Ref. 12 and $r_c = 3\sigma$ in Ref. 13. In this work, three different distance criteria were employed: $r_c = \lambda_B$ and $r_c = \lambda_B/2$ are obvious candidates, for the reasons outlined in Section II; and $r_c = 2\sigma$, in line with earlier studies.⁴¹ Using these criteria, α is the proportion of ions clustered with at least one other ion.

In addition, outlined here is a method of estimating the degree of association α from simulation data without having to specify a cluster criterion. Consider the nearest-neighbour cation-anion distribution function $p(r)$, reflecting the distance between an ion and its nearest neighbour of opposite charge. If a cation is dissociated, then the nearest-neighbour anion is remote (due to the low densities of interest here) and to a first approximation can be assumed completely uncorrelated with the cation. The probability of an anion being at a distance between r and $r + dr$ from the cation, and the remaining $N/2 - 1$ anions

being at least as far away, is

$$p_d(r)dr = \frac{N}{2} \times \frac{4\pi r^2 dr}{V} \times \left(1 - \frac{4\pi r^3}{3V}\right)^{N/2-1} \approx 2\pi\rho r^2 \exp\left(-\frac{2}{3}\pi\rho r^3\right)dr \quad (8)$$

where the subscript ‘d’ denotes ‘dissociated’. Note that $p_d(r)$ is normalised and shows a peak at $r_0 = (1/\pi\rho)^{1/3}$. If the nearest-neighbour anion is associated with the cation, then the radial distribution function $g_{+-}(r)$ will be peaked near $r = \sigma$, signalling very strong, short-range correlations which are not amenable to an accurate theoretical treatment; the corresponding function for associated (‘a’) cations, $p_a(r)$, is not easy to predict. For the RPM the arguments above apply in exactly the same way to anions. If the proportion of associated ions is α , and that of dissociated ions is $(1 - \alpha)$, then the total $p(r)$ will be given by

$$p(r) = \alpha p_a(r) + (1 - \alpha)p_d(r). \quad (9)$$

This function can be obtained directly from simulations and, in principle, fitting Eq. (9) to simulation results yields the degree of association without having to specify a cluster criterion. In practice, and without a reliable expression for $p_a(r)$, $(1 - \alpha)p_d(r)$ is fitted to $p(r)$ over the range $r \geq r_0$, where $\alpha p_a(r)$ makes no significant contribution:

$$p(r) \simeq (1 - \alpha) \left[2\pi\rho r^2 \exp\left(-\frac{2}{3}\pi\rho r^3\right)\right] \quad r > r_0. \quad (10)$$

IV. RESULTS

A. Restricted primitive model

Figure 1 shows the degree of association α as a function of reduced ion density ρ^* along several isotherms, $T^* = 0.04, 0.05, 0.06,$ and 0.07 . Recall that the critical temperature of the RPM is $T_c^* \simeq 0.05$. Four sets of simulation data are shown, corresponding to different clustering criteria. The simulation data in Figs. 1(a)-(c) were obtained using distance-based criteria of $r_c = \lambda_B, \lambda_B/2,$ and 2σ ; the data in Fig. 1(d) were obtained from fits to $p(r)$. Also included in the figures are the theoretical predictions of Eq. (5) with K evaluated numerically using Eq. (3) and $r_c = \lambda_B/2$, and with the asymptotic expression in Eq. (7). On the scale of these plots, curves with $r_c = \lambda_B$ are indistinguishable from those with $r_c = \lambda_B/2$ and so they are omitted.

The first impression given by Fig. 1 is that there is very good overall agreement between the simulation results and the theoretical predictions. A close inspection of Figs. 1(a)-(c) shows that, in simulations, the distance criteria $r_c = \lambda_B$ and $\lambda_B/2$ give slightly poorer results for the degree of association; looking at Figs. 1(a) and (b), the data along the higher temperature isotherms vary a little too sharply and saturate at $\alpha = 1$ prematurely as the density is increased. Figure 1(c) shows that the fixed-distance cut-off of $r_c = 2\sigma$ provides a more realistic variation with density, reflecting a strong association of ions in clusters close to contact.

Further insights are afforded by simulation measurements of the nearest-neighbour cation-anion distribution function, $p(r)$. Two examples from the $T^* = 0.05$

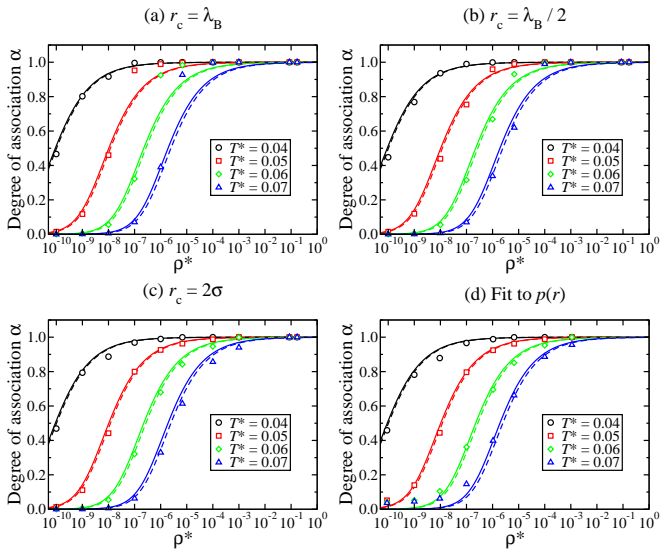


FIG. 1: The degree of association α along isotherms. The curves are the theoretical predictions of Eq. (5) using K computed with a cut-off $r_c = \lambda_B/2$ (solid lines), and using the asymptotic result in Eq. (7) for K (dashed lines). The points are the simulation results computed using various criteria: (a) distance criterion with $r_c = \lambda_B$; (b) distance criterion with $r_c = \lambda_B/2$; (c) distance criterion with $r_c = 2\sigma$; (d) fitting Eq. (10) to $p(r)$.

isotherm are shown in Fig. 2, at densities of $\rho^* = 1.05 \times 10^{-6}$ and 1.00×10^{-4} . The key point is that at these low densities, $p(r)$ appears to be a superposition of two parts: a short-range associated-ion contribution, which dies off by about $r = 2-3\sigma$; and a peaked contribution corresponding to free ions. The short-range part decays within a distance much shorter than the Bjerrum length commonly used as a distance-based clustering criterion, which at this temperature is 20σ . Assuming no correlations between free ions and any other ions in the system, the peaks in $p(r)$ should occur at $r_0 \simeq 67\sigma$ and 15σ for $\rho^* = 1.05 \times 10^{-6}$ and 1.00×10^{-4} , respectively; by comparison with the simulation results, these predictions are very reliable. The free-ion peaks are very broad, showing that a distance-based criterion $r_c \sim \lambda_B$ is not physically justified.¹² As the density of ions is increased, the peak both shifts to lower values of r and decreases in height. Equation (10) provides excellent fits to the simulation results for $p(r)$ (for $r > r_0$), and yields values for the degree of association α as shown in Fig. 1(d). There is very good agreement with the simulation results using $r_c = 2\sigma$, in correspondence with the comments made above regarding the decomposition of $p(r)$ in to a short-ranged associated-ion contribution and a broad free-ion contribution. Accordingly, there is excellent agreement between the theoretical predictions for α and the results of the analysis of $p(r)$.

Figure 1 shows that the theoretical predictions are not very sensitive to the precise values of r_c and hence K . This is explored further in Fig. 3, which shows K as a function of temperature evaluated using Eq. (3) with $r_c = \lambda_B$ and $\lambda_B/2$, and from the asymptotic expression in Eq. (7). The first two expressions give essentially identical numerical results over the temperature range $0.04 \leq T^* \leq 0.10$, the region of current interest. The asymptotic expression, Eq. (7), is accurate only at

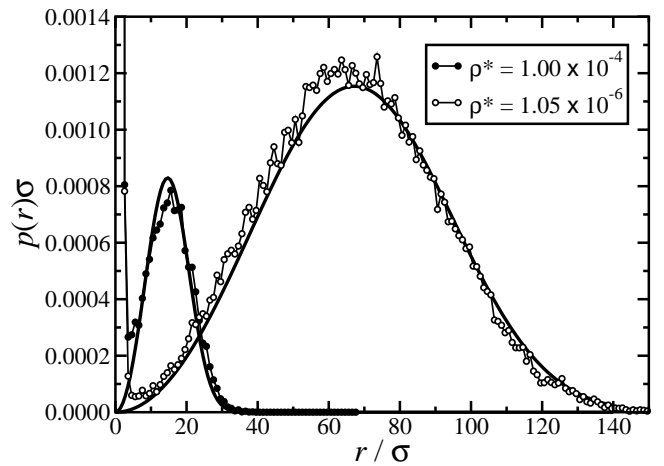


FIG. 2: Nearest-neighbour distribution function $p(r)$ at $T^* = 0.05$. The simulation results are from simulations with $\rho^* = 1.05 \times 10^{-6}$ (open symbols) and $\rho^* = 1.00 \times 10^{-4}$ (filled symbols); the thick curves are fits using the dissociated-ion result in Eq. (10) over the range $r > r_0$, where r_0 is the maximum in $p(r)$.

the lower end of the temperature range. Note that K is plotted on a logarithmic scale; the deviation between the ‘Bjerrum length’ and asymptotic results at $T^* = 0.07$ is about 20%.

When considering the effective interactions between charged colloids, it is of primary importance to know the degree of association of counterions and added salt within the suspending phase.^{9,11–14} Of course, detailed calculations are easily performed using the prescriptions outlined herein. For a qualitative assessment, however, it is useful to divide the phase diagram into regions where the ions are mostly dissociated ($\alpha < \frac{1}{2}$) and where they are mostly associated ($\alpha > \frac{1}{2}$). Within the theory outlined in Section II, the dividing line is defined by Eq. (6). The phase diagram in the ρ^*-T^* plane is shown in Fig. 4; the vapour-liquid coexistence data are taken from Ref. 22. The $\alpha = \frac{1}{2}$ line is shown for the three expressions for K , with $r_c = \lambda_B$ and $\lambda_B/2$, and from Eq. (7). The deviations between these expressions become more pronounced as temperature increases, due to the increasingly signifi-

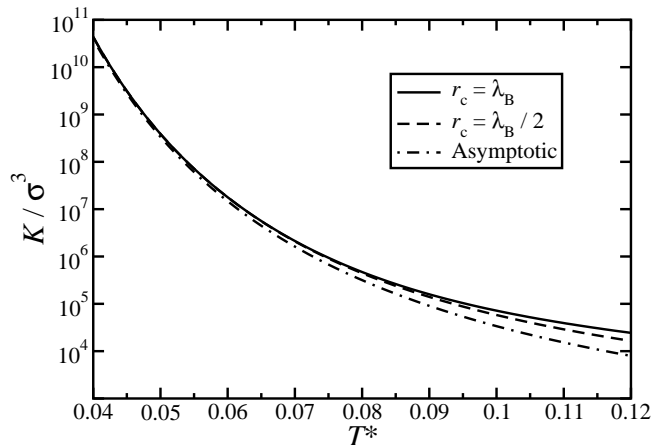


FIG. 3: Cation-anion configurational integral, K , as a function of temperature T^* : Eq. (3) with $r_c = \lambda_B$ (solid line); Eq. (3) with $r_c = \lambda_B/2$ (dashed line); Eq.(7) (dot-dashed line).

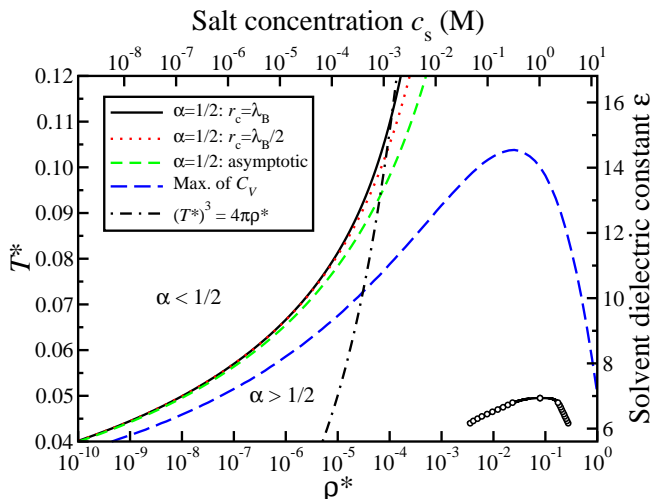


FIG. 4: Phase diagram of the RPM showing the vapour-liquid coexistence region (lower right) from simulations,²² and the boundary between dissociated ($\alpha < \frac{1}{2}$) and associated ($\alpha > \frac{1}{2}$) regimes as predicted from Eq. (6) with three different evaluations of K : Eq. (3) with $r_c = \lambda_B$ (black solid line) and $r_c = \lambda_B/2$ (red dotted line); Eq. (7) (green short-dashed line). Also shown is the locus of maxima in the constant-volume heat capacity C_V from a simple two-particle theory³⁰ (blue long-dashed line) and the boundary between ideal and strongly correlated regimes predicted by DH theory from Eq. (12) (black dot-dashed line). Real units are shown for a monovalent salt with ionic diameter $\sigma = 4 \text{ \AA}$ at a temperature $T = 298.15 \text{ K}$.

cant large- r contributions to the integral in Eq. (3).

It should be noted that significant improvements on the non-interacting particle theory are possible, and indeed have been developed in detail. Already in 1926, Bjerrum took account of the reduction in free-ion concentration in order to compute the mean activity coefficients in electrolyte solutions.^{16,36} Fisher and Levin have explored the consequences of this level of approximation on the thermodynamics and phase behaviour of the RPM in their Debye-Hückel-Bjerrum theory, and found that it leads to a vapour-liquid coexistence curve of the incorrect shape.^{19,20} Including ion-ion pair (ion-dipole) interactions restores the correct shape of the coexistence curve, and yields quite accurate values for the critical parameters. These extensions are not applied here to the problem of ion pairing: as Figs. 1(c) and (d) show, the agreement between theory and simulation at the low concentrations and low temperatures of interest is excellent; the simplest ion-pairing theory is clearly adequate for the present purposes.

The DH expression for the osmotic pressure of the electrolyte, in RPM reduced units, reads^{20,42,43}

$$\begin{aligned} \frac{\Pi\sigma^3}{k_B T} &= \frac{1}{4\pi} \left[x^2 T^* + \ln(1+x) - x + \frac{x^2}{2(1+x)} \right] \\ &\approx \rho^* \left(1 - \frac{x}{6T^*} + \dots \right) \end{aligned} \quad (11)$$

where $x = \kappa_D \sigma = \sqrt{4\pi\rho^*/T^*}$ and κ_D^{-1} is the Debye screening length. This expression is exact to leading order in x as $\rho^* \rightarrow 0$. At low density and high temperature, the ions are largely dissociated and the thermodynamics is essentially ideal. Significant deviations from ideality are expected when $x/T^* \sim 1$, and a dividing line between free-ion and strongly correlated regimes can therefore be

defined by

$$T^* = \sqrt[3]{4\pi\rho^*}. \quad (12)$$

This line is included in Fig. 4, and shows that there is a significant portion of the phase diagram in which the DH theory would suggest a low degree of ion association (because $x/T^* < 1$), but the simulations and the Bjerrum theory show that $\alpha > \frac{1}{2}$. This has a serious consequence for linearised Poisson-Boltzmann theories of electrolyte solutions and related systems, which assume weak ion-ion correlations; in that part of the phase diagram lying between the lines defined by Eqs. (6) and (12), ions are associated and hence strongly correlated despite the fact that $x/T^* < 1$.

There is one more feature of the $\alpha = \frac{1}{2}$ locus to be discussed, and that is its monotonic variation with density. At high enough density, the distinction between two free ions and one ion pair becomes blurred. At the simplest level, this volume effect can be captured by a two-particle theory, in which all ions are resolved into cation-anion pairs, and each ion pair has an internal configurational integral given by

$$q_2 = 4\pi \int_{\sigma/2}^{s_c} s^2 \exp\left(-\frac{\sigma}{2sT^*}\right) ds \quad (13)$$

where s is the distance from the ion-pair center of mass to one of the constituent ions, and the upper limit $s_c = (3/2\pi\rho)^{1/3}$ fixes the volume per pair to be $2/\rho$. Although the degree of association is not defined within this theory, one can delineate the boundary between dissociated and associated regimes with the locus of maxima in the constant-volume heat capacity $C_V = k_B \beta^2 (\partial^2 \ln q_2 / \partial \beta^2)_V$, where $\beta = 1/k_B T$.³⁰ This line is shown in Fig. 4 and suggests that the domain of associated ions is bounded from above ($T^* \simeq 0.1$). This is in correspondence with the types of phase diagrams proposed for a wide range of ionic fluids.¹⁸ It was shown in earlier work that the two-particle theory provides an excellent account of simulation measurements for the maxima in C_V .³⁰

B. Analysis of experimental data

To aid comparisons with experimental systems, axes in Fig. 4 are also shown with real units for an electrolyte with ionic diameter $\sigma = 4 \text{ \AA}$ at a temperature $T = 298.15 \text{ K}$. The concentration c_s is given in moles of salt (not ions) per litre, and with the physical temperature held constant, T^* becomes proportional to the solvent dielectric constant ϵ .

To effect a direct comparison between experiment and theory (and therefore to link experiment with simulation), attention is turned to the degree of association, α . This can be extracted from experimental measurements of the molar conductivity. Ignoring the formation of ion triples and higher charged clusters, $\alpha = 1 - \Lambda/\Lambda_0$ where Λ is the molar conductivity and Λ_0 is its limiting value at infinite dilution. The most common source of experimental uncertainty is in the determination of Λ_0 , since a suitable model has to be used to extrapolate Λ to infinite dilution. For the present purposes, conductivity data for tetraalkylammonium salts in various solvents are

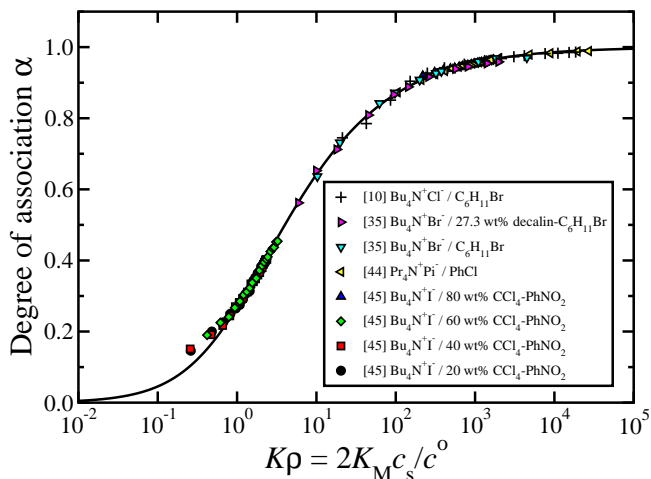


FIG. 5: Degree of association α against $K\rho = 2K_M c_s / c^\ominus$ for some tetraalkylammonium salts in various solvents. References for the experimental data are given in square brackets. The solid line is Eq. (5). (Bu =butyl, Pr =propyl, Pi =picrate.)

analysed using the quoted estimates for Λ_0 . In particular, Leunissen and co-workers have obtained the degree of association of tetrabutylammonium halides in bromocyclohexane and decalin-bromocyclohexane mixtures.^{10,35} Conductivity data for tetrapropylammonium picrate in chlorobenzene⁴⁴ and tetrabutylammonium iodide in carbon tetrachloride-nitrobenzene mixtures⁴⁵ are also analysed. The system parameters are summarised in Table I; the experimental data span wide ranges of concentration and solvent dielectric constant.

The experimental results for α are fitted using Eq. (5), with the association constant as a fitting parameter. In fact, for the purposes of analysis, $K\rho$ is replaced by $2K_M c_s / c^\ominus$, where K_M is the dimensionless ion-pairing equilibrium constant (defined on the molar scale), $2c_s$ is the ion concentration in M, and $c^\ominus = 1$ M. The fitted values of K_M are reported in Table I. The experimental values for α are shown in Fig. 5, plotted against $K\rho = 2K_M c_s / c^\ominus$. There is an impressive collapse of the experimental data on to the theoretical universal curve given by Eq. (5).

It is possible to convert the experimental parameters in to RPM units. Since q , ϵ , T , and hence λ_B are all known, an effective ion diameter σ can be obtained by equating the fitted values of K_M with the expression for K in Eq. (3), the numerical conversion between the two being

$$K = \frac{K_M}{1000 N_A c^\ominus} \quad (14)$$

where N_A is Avogadro's number. The integrand in Eq. (3) is $r^2 \exp(\lambda_B / r)$, and $r_c = \lambda_B / 2$. (Other sensible choices for r_c give essentially the same numerical results.) The ion diameter σ is obtained by numerical solution of Eq. (3). This procedure ignores chemical detail such as the precise nature of the short-range repulsive interactions and the presence of van der Waals interactions, and so the fitted values of σ might reflect some non-coulombic effects. Nonetheless, under the conditions considered here, the coulombic interaction between ions at contact is dominant (being in the range of 10-20 $k_B T$)

and so the effective RPM parameters are expected to be meaningful.

Values of λ_B , σ , $T^* = \sigma / \lambda_B$, and the range of RPM ion densities ρ^* are all summarised in Table I. The data of Leunissen and co-workers correspond to RPM temperatures in the region of $T^* = 0.05$, and RPM ion densities as low as $\rho^* = 10^{-8}$; Lindbäck and Beronius' data⁴⁴ correspond to a similar temperature, but do not extend to as low concentration. The data of Roy *et al.*⁴⁵ do not extend to very low concentration, but they do span the temperature range $0.06 \leq T^* \leq 0.11$. Note that the experimental data correspond to the regime where the mean ion-ion separation ($\rho^{-1/3}$) is much greater than the Bjerrum length, i.e., in RPM units $\sqrt[3]{4\pi\rho^*} \ll T^*$. This corresponds to the weakly interacting regime of the DH theory summarised in Section IV A, and so the theory would not have predicted the extensive pairing apparent in experiments. The central conclusion is that the Bjerrum theory (and by association, the simulations) successfully treats the ion-pairing equilibrium of nanomolar salt solutions in low-polarity solvents, such as those employed in recent work on charged-colloid suspensions.²⁻¹¹

The effects of ion pairing on the effective screening length will now be considered. The appropriate effective screening parameter in the presence of association is clearly

$$\kappa = \sqrt{4\pi(1-\alpha)\rho\lambda_B} = \kappa_D \sqrt{1-\alpha} \quad (15)$$

where $\kappa_D = \sqrt{4\pi\rho\lambda_B}$ is the inverse of the Debye length. At very low salt concentrations where $K\rho \ll 1$, Eq. (5) shows that $\alpha \approx \frac{1}{2}K\rho$, and hence

$$\frac{\kappa}{\kappa_D} \approx 1 - \frac{1}{4}K\rho. \quad (16)$$

The screening length is then essentially equal to that assuming complete dissociation, i.e., the Debye length. At higher concentrations where $K\rho \gg 1$, Eq. (5) predicts $\alpha \approx 1 - \sqrt{2/K\rho}$ and hence

$$\frac{\kappa}{\kappa_D} \approx \left(\frac{2}{K\rho} \right)^{1/4}. \quad (17)$$

In this regime, $\kappa \ll \kappa_D$ and hence the screening length is much longer than would be expected on the basis of complete dissociation. Moreover, there is an unusual scaling behaviour: because κ_D has a $\rho^{1/2}$ dependence, the effective scaling parameter scales like $\kappa \sim \rho^{1/2} \cdot \rho^{-1/4} = \rho^{1/4}$. Hence, the effective screening length scales like $\kappa^{-1} \sim \rho^{-1/4}$, while the Debye length scales like $\kappa_D^{-1} \sim \rho^{-1/2}$.

A glance at Fig. 5 shows that the regime $K\rho \gg 1$ is in fact experimentally accessible. In particular, the experimental measurements by Leunissen and co-workers^{10,35} extend to a very high degree of association, and so the resulting interactions between charged colloids suspended in these solutions will not be screened as effectively as might be expected. As an example, Fig. 6 shows the Debye length $\kappa_D^{-1} \propto c_s^{-1/2}$, and the effective screening length κ^{-1} from Eq. (15), for a solution with $\sigma = 4$ Å, $\epsilon = 7$, and $T = 298.15$ K; this set of parameters corresponds to a reduced RPM temperature of $T^* = 0.05$, and is representative of experiments in low-polarity solvents. Over the range 10^{-9} M $\leq c_s \leq 10^{-7}$ M, the screening length and the Debye length coincide, ranging from several micrometres down to several hundred nanometres; these

TABLE I: Physical parameters for tetraalkylammonium salts in various solvents: ϵ is the solvent dielectric constant, λ_B is the Bjerrum length for $T = 298.15$ K, c_s is the salt concentration, K_M is the dimensionless ion-pairing association constant (defined on the molar scale), and σ is the effective hard-sphere diameter of the ion. $T^* = \sigma/\lambda_B$ and ρ^* are the effective RPM temperature and density, respectively. (Bu =butyl, Pr =propyl, Pi =picrate.)

System	Ref.	ϵ	λ_B (Å)	c_s (μM)	K_M	σ (Å)	T^*	$10^6 \rho^*$
$\text{Bu}_4\text{N}^+\text{Cl}^- / \text{C}_6\text{H}_{11}\text{Br}$	10	7.92	70.8	0.28–244	3.80×10^7	3.27	0.0462	0.0118–10.3
$\text{Bu}_4\text{N}^+\text{Br}^- / \text{C}_6\text{H}_{11}\text{Br}$	35	7.92	70.8	0.56–245	9.17×10^6	3.57	0.0504	0.0307–13.4
$\text{Bu}_4\text{N}^+\text{Br}^- / 27.3 \text{ wt\% decalin-C}_6\text{H}_{11}\text{Br}$	35	5.62	99.7	0.47–157	6.31×10^6	5.53	0.0555	0.0957–32.0
$\text{Pr}_4\text{N}^+\text{Pi}^- / \text{PhCl}$	44	5.612	99.9	5.97–1539	8.80×10^6	5.41	0.0542	1.14–294
$\text{Bu}_4\text{N}^+\text{I}^- / 80 \text{ wt\% CCl}_4\text{-PhNO}_2$	45	10.22	54.8	170–1330	6.44×10^5	3.16	0.0576	6.46–50.5
$\text{Bu}_4\text{N}^+\text{I}^- / 60 \text{ wt\% CCl}_4\text{-PhNO}_2$	45	17.45	32.1	170–1320	1.23×10^3	3.17	0.0987	6.52–50.6
$\text{Bu}_4\text{N}^+\text{I}^- / 40 \text{ wt\% CCl}_4\text{-PhNO}_2$	45	23.90	23.5	440–4070	2.91×10^2	2.60	0.111	9.31–86.2
$\text{Bu}_4\text{N}^+\text{I}^- / 20 \text{ wt\% CCl}_4\text{-PhNO}_2$	45	29.66	18.9	830–7380	1.57×10^2	2.08	0.110	9.00–80.0

values correspond well with experimentally determined values.^{8,9} At higher salt concentrations $c_s > 10^{-7}$ M, κ^{-1} exceeds κ_D^{-1} due to the formation of ion pairs. In addition, κ^{-1} decays less fast with increasing concentration, switching over to the $c_s^{-1/4}$ dependence advertised in Eq. (17). Finally, it is noted that at very high concentrations (outwith the relevant range studied here) the formation of ion pairs can lead to κ^{-1} increasing with increasing c_s ; the ion-pair contribution to the effective dielectric constant of the solution increases with increasing concentration, which ultimately leads to reductions in λ_B and κ .¹⁴

Some interesting transient behaviour has been observed in experiments on charged-colloid suspensions.³ Specifically, the colloids show the effects of anomalously long-ranged repulsions which are incompatible with the apparent salt concentration $c_s \sim 10^{-8}$ M. This transient behaviour can occur on the timescale of a few days. One contributing factor might be the time taken for ions to associate and/or dissociate after preparation. For instance, if ions were initially associated, then the screening length and colloidal repulsions would decrease on the approach to equilibrium. Assuming that the association of cations with anions is a second-order, diffusion-controlled ‘reaction’, then the corresponding macroscopic rate constant

can be estimated by $k_a = 8RT/3\eta$,⁴⁶ where η is the viscosity of the solvent. For a solvent with $\eta = 10^{-3}$ Pa s at room temperature, this yields $k_a = 7 \times 10^9 \text{ M}^{-1} \text{ s}^{-1}$. The corresponding first-order dissociation of ion pairs will have a rate constant $k_d = k_a c^\ominus / K_M$. Table I shows that K_M can be as high as 10^7 , and so the characteristic time for ion dissociation will be no more than $1/k_d \sim 0.001$ s. This is only a very rough estimate and solvation-shell structure and the slow escape from the long-range coulombic attraction between ions may well increase this timescale considerably, but it seems unlikely that ion dissociation is the dominant cause of the transient behaviour. A more prosaic explanation for the observed transients in Ref. 3 may be that ions are initially sequestered but subsequently released by impurities such as water or by the container walls, leading to a slow reduction in the screening length.

V. CONCLUSIONS

In this paper, the association of ions in low-polarity solvents was studied within the context of the restricted primitive model at low concentration and low temperature. In reduced units, concentrations as low as 10^{-10} and temperatures as low as 0.04 were simulated using an efficient Monte Carlo algorithm,²¹ and comparisons were made with Bjerrum’s quasi-chemical ion-pairing theory.¹⁶ These conditions correspond to nanomolar salt solutions in low dielectric constant solvents under ambient conditions; such media are of relevance to recently synthesised charged-colloid suspensions.^{2–11} The degree of ion association strongly affects the effective interactions between colloids,^{12–14} and so one of the aims of this work was to map out the different regimes of association on the phase diagram.

In the simulations, distance-based criteria and the nearest-neighbour cation-anion distribution function $p(r)$ were used to determine the degree of association. It was shown that conventional distance-based criteria based on the Bjerrum length¹² are inferior to a short-range cutoff.^{13,41} This conclusion was backed up by analysis of $p(r)$, which shows that associated ions are in close proximity, while free ions show a very broad distribution of distances to the nearest ion of opposite charge.

To some extent, this feature is accounted for in theoretical treatments based on an ion-pair configurational integral, since it is the Boltzmann factor at short-range

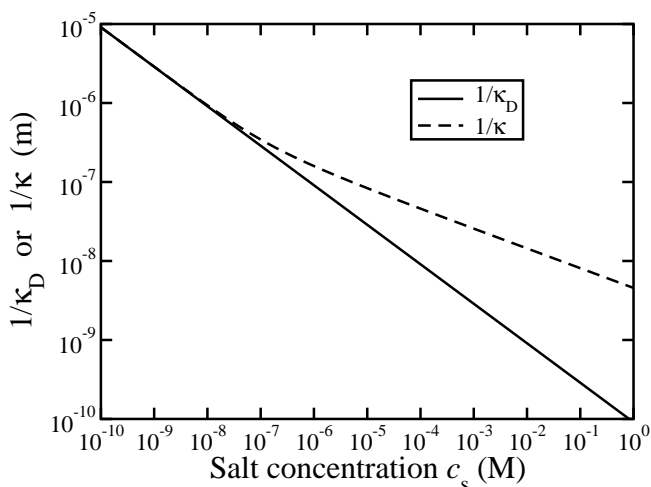


FIG. 6: The Debye length κ_D^{-1} , and the effective screening length κ^{-1} from Eq. (15), for a solution with $\sigma = 4$ Å, $\epsilon = 7$, and $T = 298.15$ K; this set of parameters corresponds to a reduced RPM temperature of $T^* = 0.05$.

which makes the most significant contribution, at least at low temperatures where association is prevalent. The precise value of the upper limit in the integral is not important, as already noted long ago.³⁶ The agreement between Bjerrum theory and simulation under the physical conditions studied here is excellent. More sophisticated treatments, such as those developed by Fisher and Levin,^{19,20} are scarcely required; of course, near to the coexistence region, ion-ion and ion-dipole interactions become of paramount importance. Additionally, the analysis of experimental dielectric and conductivity data at low temperature and moderate concentrations requires a detailed account of ion triples and higher (charged) clusters;¹⁵ such phenomena as conductivity minima in the vicinity of the coexistence region can be handled using suitable extensions of the DH theory that include the effects of association.^{47,48}

A comparison of the Bjerrum theory and the Debye-Hückel theory shows that there is a significant region of the phase diagram where the former predicts strong ion association (in agreement with simulations) but the latter indicates only weak ion-ion correlations. This implies that linearised Poisson-Boltzmann theories, which assume weak ion-ion correlations, should only be applied under conditions where ion association is actually known to be insignificant. Those conditions are identified in this work. Of course, these restrictions should also be observed in the application of the Derjaguin-Landau-Verwey-Overbeek theory because it incorporates Debye screening of colloidal interactions under the assumption of weak ion-ion correlations, at least for the case of spherical colloidal particles.

The Bjerrum theory was compared with experimental

data for tetraalkylammonium salts in low-polarity solvents, and the agreement was found to be excellent. Fitting the association constants allowed a mapping between real systems and the restricted primitive model. Simulation, theory, and experiment have therefore been compared at very low concentrations and low temperatures. One of the primary motivations for this study was to understand the association of ions in low-polarity solvents, with a view to getting a clear picture of the nature of screening between colloidal particles suspended in such solutions. The effects of ion association on the appropriate screening lengths have been quantified, and the results are in complete accord with experiment. It is hoped that the results presented herein can be used in subsequent treatments of charged-colloid interactions in low-polarity media.

Acknowledgments

The authors thank Dr Mirjam E. Leunissen and Dr Andrew D. Hollingsworth for communicating the results of Ref. 35 prior to publication, and Dr Leunissen and the anonymous referees for useful comments and suggestions. M. D. and C. V. acknowledge a NWO-VICI grant which supported the early stages of this work. C. V. acknowledges financial support from EPSRC grant EP/E030173, and from the European Union through an Individual Inter-European Marie Curie Fellowship. This work has made use of the resources provided by the Edinburgh Compute and Data Facility (ECDF). The ECDF is partially supported by the eDIKT initiative.

* Corresponding author: philip.camp@ed.ac.uk

¹ E. J. W. Verwey and J. T. G. Overbeek, *Theory of the stability of lyophobic colloids*, Elsevier, Amsterdam, 1948.
² A. Yethiraj and A. van Blaaderen, *Nature*, 2003, **421**, 513–517.
³ C. P. Royall, M. E. Leunissen, and A. van Blaaderen, *J. Phys.: Condens. Matter*, 2003, **15**, S3581–S3596.
⁴ M. E. Leunissen, C. G. Christova, A.-P. Hynninen, C. P. Royall, A. I. Campbell, A. Imhof, M. Dijkstra, R. van Roij, and A. van Blaaderen, *Nature*, 2005, **437**, 235–240.
⁵ A. I. Campbell, V. J. Anderson, J. S. van Duijneveldt, and P. Bartlett, *Phys. Rev. Lett.*, 2005, **94**, 208301.
⁶ E. V. Shevchenko, D. V. Talapin, N. A. Kotov, S. O’Brien, and C. B. Murray, *Nature*, 2006, **439**, 55–59.
⁷ P. J. Lu, J. C. Conrad, H. M. Wyss, A. B. Schofield, and D. A. Weitz, *Phys. Rev. Lett.*, 2006, **96**, 028306.
⁸ M. E. Leunissen, A. van Blaaderen, A. D. Hollingsworth, M. T. Sullivan, and P. M. Chaikin, *Proc. Natl. Acad. Sci. (USA)*, 2007, **104**, 2585–2590.
⁹ M. E. Leunissen, J. Zwanikken, R. van Roij, P. M. Chaikin, and A. van Blaaderen, *Phys. Chem. Chem. Phys.*, 2007, **9**, 6405–6414.
¹⁰ M. E. Leunissen *Manipulating colloids with charges and electric fields* PhD thesis, Utrecht University, 2007.
¹¹ J. Zwanikken and R. van Roij, *Phys. Rev. Lett.*, 2007, **99**, 178301.
¹² E. Allahyarov, E. Zaccarelli, F. Sciortino, P. Tartaglia, and H. Löwen, *Europhys. Lett.*, 2007, **78**, 38002.
¹³ E. Allahyarov, E. Zaccarelli, F. Sciortino, P. Tartaglia, and H. Löwen, *Europhys. Lett.*, 2008, **81**, 59901.

¹⁴ J. Zwanikken and R. van Roij, *J. Phys.: Condens. Matter*, 2009, **21**, 424102.
¹⁵ R. A. Robinson and R. H. Stokes, *Electrolyte solutions*, Butterworths, London, 2nd ed., 1959.
¹⁶ N. Bjerrum, *Kgl. Dan. Vidensk. Selsk. Mat.-fys. Medd.*, 1926, **7**, 1–48.
¹⁷ K. S. Pitzer, *J. Phys. Chem.*, 1984, **88**, 2689–2697.
¹⁸ K. S. Pitzer, *Acc. Chem. Res.*, 1990, **23**, 333–338.
¹⁹ M. E. Fisher and Y. Levin, *Phys. Rev. Lett.*, 1993, **71**, 3826–3829.
²⁰ Y. Levin and M. E. Fisher, *Physica A*, 1996, **225**, 164–220.
²¹ C. Valeriani, P. J. Camp, J. W. Zwanikken, R. van Roij, and M. Dijkstra, *J. Phys.: Condens. Matter*, 2010, **22**, 104122.
²² J. M. Romero-Enrique, L. F. Rull, and A. Z. Panagiotopoulos, *Phys. Rev. E*, 2002, **66**, 041204.
²³ C. Vega, J. L. F. Abascal, C. McBride, and F. Bresme, *J. Chem. Phys.*, 2003, **119**, 964–971.
²⁴ J.-M. Caillol, D. Levesque, and J.-J. Weis, *J. Chem. Phys.*, 2002, **116**, 10794–10800.
²⁵ E. Luijten, M. E. Fisher, and A. Z. Panagiotopoulos, *Phys. Rev. Lett.*, 2002, **88**, 185701.
²⁶ J. P. Valleau, L. K. Cohen, and D. N. Card, *J. Chem. Phys.*, 1980, **72**, 5942.
²⁷ M. J. Gillan, *Molec. Phys.*, 1983, **49**, 421–442.
²⁸ J. M. Caillol, *J. Chem. Phys.*, 1995, **102**, 5471–5479.
²⁹ F. Bresme, E. Lomba, J.-J. Weis, and J. L. F. Abascal, *Phys. Rev. E*, 1995, **51**, 289–296.
³⁰ P. J. Camp and G. N. Patey, *Phys. Rev. E*, 1999, **60**, 1063–1066.

- ³¹ P. J. Camp and G. N. Patey, *J. Chem. Phys.*, 1999, **111**, 9000–9008.
- ³² J. C. Shelley and G. N. Patey, *J. Chem. Phys.*, 1995, **103**, 8299–8301.
- ³³ C. D. Daub, G. N. Patey, and P. J. Camp, *J. Chem. Phys.*, 2003, **119**, 7952–7956.
- ³⁴ G. Ganzenmüller and P. J. Camp, *J. Chem. Phys.*, 2007, **126**, 191104.
- ³⁵ A. D. Hollingsworth, M. E. Leunissen, A. Yethiraj, A. van Blaaderen, and P. Chaikin, unpublished work.
- ³⁶ R. Fowler and E. A. Guggenheim, *Statistical Thermodynamics*, Cambridge University Press, Cambridge, 1956.
- ³⁷ P. C. Jordan, *Mol. Phys.*, 1973, **25**, 961–973.
- ³⁸ W. Ebeling, *Z. Phys. Chem.*, 1968, **238**, 400–402.
- ³⁹ G. Orkoulas and A. Z. Panagiotopoulos, *J. Chem. Phys.*, 1994, **101**, 1452–1459.
- ⁴⁰ M. P. Allen and D. J. Tildesley, *Computer simulation of liquids*, Clarendon Press, Oxford, 1987.
- ⁴¹ J.-M. Caillol and J.-J. Weis, *J. Chem. Phys.*, 1995, **102**, 7610–7621.
- ⁴² P. Debye and E. Hückel, *Phys. Z.*, 1923, **24**, 185–206.
- ⁴³ D. A. McQuarrie, *Statistical mechanics*, Harper-Collins, New York, 1976.
- ⁴⁴ T. Lindbäck and P. Beronius, *Acta Chem. Scand. A*, 1980, **34**, 709–715.
- ⁴⁵ M. N. Roy, P. K. Roy, R. S. Sah, P. Pradhan, and B. Sinha, *J. Chem. Eng. Data*, 2009, **54**, 2429–2435.
- ⁴⁶ P. Atkins and J. de Paula, *Atkins' Physical Chemistry*, Oxford University Press, Oxford, 9th ed., 2010.
- ⁴⁷ H. Weingärtner, V. C. Weiss, and W. Schröer, *J. Chem. Phys.*, 2000, **113**, 762–770.
- ⁴⁸ W. Schröer and H. Weingärtner, *Pure Appl. Chem.*, 2004, **76**, 19–27.

Figure captions

- Fig. 1** The degree of association α along isotherms. The curves are the theoretical predictions of Eq. (5) using K computed with a cut-off $r_c = \lambda_B/2$ (solid lines), and using the asymptotic result in Eq. (7) for K (dashed lines). The points are the simulation results computed using various criteria: (a) distance criterion with $r_c = \lambda_B$; (b) distance criterion with $r_c = \lambda_B/2$; (c) distance criterion with $r_c = 2\sigma$; (d) fitting Eq. (10) to $p(r)$.
- Fig. 2** Nearest-neighbour distribution function $p(r)$ at $T^* = 0.05$. The simulation results are from simulations with $\rho^* = 1.05 \times 10^{-6}$ (open symbols) and $\rho^* = 1.00 \times 10^{-4}$ (filled symbols); the thick curves are fits using the dissociated-ion result in Eq. (10) over the range $r > r_0$, where r_0 is the maximum in $p(r)$.
- Fig. 3** Cation-anion configurational integral, K , as a function of temperature T^* : Eq. (3) with $r_c = \lambda_B$ (solid line); Eq. (3) with $r_c = \lambda_B/2$ (dashed line) (this is almost indistinguishable from the former curve, in this temperature range); Eq.(7) (dot-dashed line).
- Fig. 4** Phase diagram of the RPM showing the vapour-liquid coexistence region (lower right) from simulations,²² and the boundary between dissociated ($\alpha < \frac{1}{2}$) and associated ($\alpha > \frac{1}{2}$) regimes as predicted from Eq. (6) with three different evaluations of K : Eq. (3) with $r_c = \lambda_B$ (black solid line) and $r_c = \lambda_B/2$ (red dotted line); Eq. (7) (green short-dashed line). Also shown is the locus of maxima in the constant-volume heat capacity C_V from a simple two-particle theory³⁰ (blue long-dashed line) and the boundary between ideal and strongly correlated regimes predicted by DH theory from Eq. (12) (black dot-dashed line). Real units are shown for a monovalent salt with ionic diameter $\sigma = 4 \text{ \AA}$ at a temperature $T = 298.15 \text{ K}$.
- Fig. 5** Degree of association α against $K\rho = 2K_M c_s / c^\ominus$ for some tetraalkylammonium salts in various solvents. References for the experimental data are given in square brackets. The solid line is Eq. (5). (Bu =butyl, Pr =propyl, Pi =picrate.)
- Fig. 6** The Debye length κ_D^{-1} , and the effective screening length κ^{-1} from Eq. (15), for a solution with $\sigma = 4 \text{ \AA}$, $\epsilon = 7$, and $T = 298.15 \text{ K}$; this set of parameters corresponds to a reduced RPM temperature of $T^* = 0.05$.